

A. V. Postnikov* and P. Entel†

Gerhard Mercator University Duisburg – Theoretical Low-Temperature Physics, D-47048 Duisburg, Germany

José M. Soler‡

*Departamento de Física de la Materia Condensada,
Universidad Autónoma de Madrid, E-28049 Madrid, Spain*

(Dated: October 26, 2018)

We calculate from first principles the electronic structure, relaxation and magnetic moments of small Fe particles, by applying the numerical local orbitals method in combination with norm-conserving pseudopotentials. The accuracy of the method in describing elastic properties and magnetic phase diagrams is tested by comparing benchmark results for different phases of crystalline iron to those obtained by an all-electron method. Our calculations for the bipyramidal Fe₅ cluster confirm previous plane-wave results that predicted a non-collinear magnetic structure. For larger bcc-related (Fe₃₅, Fe₅₉) and fcc-related (Fe₃₈, Fe₄₃, Fe₅₅, Fe₆₂) particles, a larger inward relaxation of outer shells has been found in all cases, accompanied by an increase of local magnetic moments on the surface to beyond 3 μ_B .

PACS numbers: 36.40.Cg, 75.50.Bb, 71.15.-m

I. INTRODUCTION

Magnetic properties of small iron nanoparticles are often unusual and quite different from those of the bulk. Experimental information is not abundant and confined essentially to determination of mean magnetic moment, depending on the cluster size and temperature, e.g. from Stern-Gerlach deflection as measured by Billas *et al.*^{1,2} (see also Ref. 3 for a recent review on experimental situation). The morphology, structural relaxation or distribution of magnetic moments from the center to the surface are so far not accessible in experiment. The microscopic theory, on the other hand, can in principle address these issues and thus be of great help. A range of different approaches have been tried on Fe clusters, illustrating a compromise between severeness of approximations done and the size of system to be treated. The lack of symmetry is a common difficulty in all cluster studies; but Fe poses an additional challenge even among other transition-metal systems because its electronic structure and magnetic properties are known to be very sensitive to local environment. In course of the last decade, a number of simulations have been done with the use of appropriately tuned potential energy functions (see, e.g., Christensen and Cohen⁴ and Besley *et al.*⁵), or of parametrized Hubbard-type Hamiltonian, to account for magnetic properties^{6,7,8,9,10,11}. The parameterization is typically done to the data of (bulk) band structure calculation and experimental (spectroscopic) results; common approximations are the neglect of interactions beyond the first (or second) neighbors, sometimes fixed cluster geometry¹² or only topological variation of unrelaxed cluster structure, with nearest-neighbors distances fixed⁷. Those semiempirical calculations which keep track of electronic degrees of freedom and not just potential function were able to treat up to 89 (Ref. 11) – 169 (Ref. 10) – 177 (Ref. 12, in a fixed high-symmetry arrangement) Fe atoms.

First-principles simulations by means of density functional theory (DFT)¹³, while still subject to certain basic approximations, have the advantage of not being biased by a particular parameterization. Following constrained structure optimizations (for selected high-symmetry arrangements) of small (up to Fe₄) systems by Chen *et al.*¹⁴, Castro and Salahub searched for ground-state structures, and reported other related properties, of low-symmetry clusters, Fe₅ being the largest^{15,16}. Recently Kortus *et al.*¹⁷ calculated magnetic moments and anisotropy energies of (symmetric) 5-at. and 13-at. clusters of Fe-Co composition, including all-Fe case. Ballone and Jones¹⁸ optimized the structures of clusters up to Fe₇, making use of norm-conserving pseudopotentials and Car-Parrinello molecular dynamics. A similar approach, i.e. essentially a planewave simulation of a cluster in a box with implied periodic boundary conditions, has been applied in later publications by Oda *et al.*¹⁹ and Hobbs *et al.*²⁰ who concentrated on apparent non-collinearity of local magnetic moments in the ground-state structures of Fe₃ and Fe₅ clusters. The results of these two calculations, while being not quite identical, contested previous results obtained for the cluster geometry and energetics obtained by a (magnetically collinear) methods (e.g., by Gaussian orbitals technique in Ref. 16) and seem to establish a present-day margin of reliability for DFT-based calculations. A snapshot of available theoretical knowledge on transition-metal clusters as for 1999, along with relevant experimental information, can be found in a review by Alonso²¹.

While for such relatively small systems one can hope to pinpoint the ground-state geometry among several competing metastable configurations, this seems hardly feasible for larger particles, consisting of several tens or hundreds of atoms. However, in such systems some general ideas about the particles' morphology, radial distribution of density

and magnetization would be already of interest for establishing relation with measurements on particle beams, where clusters of such sizes typically participate and exhibit non-trivial variation of properties with size^{1,2}. It would be a reasonable assumption that bulk-like features, i.e. at least local neighborhood of either bcc or fcc type would emerge with increasing the particle size. Moreover, the arrangement of atoms over icosahedral shells has been detected for rare gas clusters and also comes into consideration for Ni particles (see Ref. 21 for a review). One should note that a self-consistent treatment of electronic structure over a Fe particle including several shells of atoms is a technically demanding task even for a fixed atomic arrangement, and the need for accurate total energy and forces for a structure optimization complicates this problem even further. Fujima and Yamaguchi²² performed DFT calculations by a discrete variational method for Fe₁₅ and Fe₃₅ clusters in the fixed (crystalline-like) bcc structure, that exhibited an enhancement of local magnetic moments towards the surface. Recently Duan and Zheng²³ reported magnetic moments in 13- and 55-atom clusters of Fe, Co and Ni in fcc-, hexagonal closed packed and icosahedral geometry, allowing a breathing relaxation within the DFT (for small clusters only).

The aim of the present paper is to study electronic structure and magnetism in some additional representative cluster morphologies, making use of the first-principles method within the DFT that would allow accurate evaluation of total energy differences, conjugate gradient optimization of ground-state structure without need for symmetry constraints. To this end, we apply SIESTA,^{24,25,26} an *ab initio* electronic-structure and molecular-dynamics simulation package, relying on norm-conserving pseudopotentials and strictly localized numerical pseudoatomic orbitals. This method has recently been applied to the relaxation of gold clusters, up to Au₇₅²⁷. Also, some studies have been done by Izquierdo *et al.*²⁸ on bulk and low-dimensional Fe systems (small free and deposited clusters, monolayer and nanowire)²⁸ – primarily, in the view of their magnetic properties and without structure relaxation allowed. Finally, Diéguez *et al.*²⁹ searched for ground-state structures and evaluated the average magnetic moment and other properties in the hierarchy of Fe clusters from 2 to 17 atoms.

In our simulation of larger clusters we want to be sure that the accuracy of the SIESTA method is sufficient for the adequate description of delicate structure/magnetization interplay in Fe systems. Therefore, after specifying the details of calculation we report the benchmark calculations for bcc/fcc phase diagram of bulk iron. Further on, we allow for non-collinear alignment of magnetic density in the treatment of the Fe₅ cluster as another benchmark, that is discussed afterwards in relation with previous planewave calculations on this system. In the subsequent sections, we present the results for nanoparticles (in bcc and fcc prototype structure, and with the icosahedral symmetry) not covered by previous studies, with the 62 Fe atoms as the largest.

II. COMPUTATIONAL PROCEDURE

The underlying methodology and performance of the SIESTA method has been reviewed in recent publications^{26,30,31}. The basis set consists of numerically defined strictly localized pseudoatomic orbitals. It uses norm-conserving (possibly hard) pseudopotentials and a uniform real-space grid to represent the valence charge density and to calculate the Hartree and exchange-correlation potentials and their corresponding matrix elements.

The necessary plane-wave cutoff in this charge density representation may become large, depending on the system under consideration. In many systems, e.g. those containing magnetic 3*d* elements, it turns out essential to use a pseudocore correction for the pseudopotential as proposed by Louie *et al.*³², in order to accurately recover the exchange-correlation potential due to full density, imitating the effect of the core states. A strong localization of such pseudocore for Fe demands a high charge-density cutoff (see below), that is one of the main limiting factors in the treatment of larger Fe systems (in what regards the size of the simulation cell) by SIESTA. The extension of the most diffuse basis function on Fe atom was about 6.8 a.u., and the resulting size of the simulation cell for a cluster (i.e. that would prevent direct overlap of atomic functions across the cell boundary) was 35 a.u. for the largest particle we used (Fe₆₂).

We used a double- ζ singly-polarized (DZP) basis set, with 15 orbitals per atom. This basis was discussed for Fe in Ref. 28). The pseudopotential has been generated for the [Ar]3*d*⁷ 4*s*¹ configuration (with 3*p*⁶ sometimes also participating in the pseudopotential generation, see below) and a pseudocore radius of 0.7 a.u. Other aspects of calculation were largely similar to those of Ref. 28. We note that the same calculation method but slightly different setup has been recently used by Diéguez *et al.*²⁹. The most important difference is the use of triple- ζ basis set with double- ζ polarized functions there, which is probably superior to our choice of a more compact basis. Moreover, the spatial extension of the basis functions in the calculation by Diéguez *et al.* were larger³³. The latter fact lead to a considerably larger size of the simulation cell and, with the cutoff chosen in Ref. 29, to a relatively sparse mesh for the representation of the charge density. However, we used a higher cutoff and hence more dense real-space mesh.

A part of the results of the present study deals with a general-shape (non-collinear) treatment of magnetization. Whereas its implementation in the local density approximation (LDA) may be considered as relatively straightforward, with the use of a generalized gradient approximation (GGA) the exchange-correlation energy in non-collinear case

would depend on the directions of both the magnitude and the direction of the magnetization. To our knowledge, no such full implementation has been elaborated, and the non-collinear GGA calculation of Hobbs *et al.*²⁰ was not sufficiently detailed on this point. Thus, we restrict the non-collinear calculations to LDA.

III. BENCHMARK CALCULATIONS FOR BULK IRON

The electronic structure of bulk iron is well known and can nowadays be well reproduced by different methods of density functional theory. The SIESTA method was earlier used by Izquierdo *et al.*²⁸ to study the ground state properties (equilibrium volume, bulk modulus, magnetic moment) of bcc-Fe using the GGA. A comparison with results obtained by other methods can also be found in this publication. However, two important issues of the ground state of Fe as a benchmark system of the DFT were not addressed in Ref. 28 and are discussed below. These are, a low-spin to high-spin transition with the increase of volume in fcc-Fe^{34,35}, and the necessity to go beyond the LDA in order to obtain a correct sequence of bcc–fcc ground state energies^{36,37}. The calculated energy–volume curves for different structural and magnetic phases of Fe can be found in Ref. 38. In order to check the quality of pseudopotential and basis set used in the present simulation, we compared the results obtained for bulk iron using the SIESTA code with those produced by the full-potential augmented plane-wave method, as implemented in the WIEN2k package³⁹. The energy–volume curves and magnetic moment values as calculated in the LDA for bcc and fcc ferromagnetic phases are shown in Fig. 1.

It is noteworthy that the curvatures of both bcc and fcc energy-volume functions, not only near their corresponding minima but over whole range of relevant volumes, are faithfully reproduced by SIESTA. In particular, we emphasize the low spin – high spin transition in the fcc phase (probably, reported for the first time by Moruzzi *et al.*³⁴) with a related kink in the energy – volume curve. Moreover, SIESTA accurately describes a crossover between the bcc and fcc volume curves and the (erroneous) result that the absolute energy minima occurs in the fcc phase, as is well known to be an artifact of the LDA. As regards the magnetic moments, it is encouraging that their absolute values (per atom), as calculated by SIESTA and WIEN2k, agree well in the bcc phase over all relevant range of volumes. In the fcc phase, the position, the magnitude and even a complicated profile of the low spin – high spin transition is correctly reproduced.

A similar calculation, that also included the antiferromagnetic (AFM; B2-type) phase for bcc iron, has been performed with the use of GGA (Perdew-Bourke-Ernzrhof⁴⁰ in both SIESTA and WIEN2k realizations); the results are shown in Fig. 2. The energy differences between phases at their corresponding equilibrium volumina are fairly well reproduced by SIESTA; the relative depths of two local energy minima on the fcc energy curve come out however somehow distorted.

In order to study the effect of inclusion of upper core states (Fe3*p*) in the pseudopotential generation on the equation of state, we calculated the total energy as function of volume with these states attributed either to the core or to the valence band. As can be seen in Fig. 2, the differences are noticeable for the spin-flip transition energy but almost negligible for the comparison of bcc and fcc phases. Since no equilibrium volume nor the compressibility are affected, we won't expect a big role of the Fe3*p* states included beyond the fixed core on the structure relaxation or lattice dynamics with a fixed magnetic ordering.

IV. RESULTS FOR THE Fe₅ CLUSTER

The geometry and magnetic structure of small Fe clusters (Fe₂ – Fe₅) have been recently addressed in a number of *ab initio* calculations by different methods. For Fe₃ and Fe₅, a non-collinear magnetic ordering has been reported^{19,20}. Although direct experimental justification of these theoretical prediction was apparently not yet possible, a qualitative consensus between recent high-accuracy data allows to consider these small clusters as non-trivial benchmark systems (it should be noted that spin-orbit interaction was not considered in the simulations cited, nor did we include it in our present treatment). For the linear Fe₃ cluster, we obtained the results in good agreement with the calculation of Oda *et al.*¹⁹: interatomic distance of 3.63 a.u.; magnetic moments of 3.07 μ_B (almost antiparallel but canted each by 5°) at apical Fe atoms; 1.26 μ_B (coplanar with these two and canted by 90°) on the central atom. It should be noted that Hobbs *et al.*²⁰ claim this magnetic structure to be realistic but not fully converged and unstable with respect to a fully collinear configuration. So additional studies are probably needed to clarify this controversy.

As for the Fe₅ cluster, both previous studies agree at least qualitatively on the ground-state magnetic configuration. In Table I, we summarize our results in comparison with those of Refs. 19,20 for collinear and non-collinear arrangement of local moments. In our calculations, the simulation cell of the dimensions 12×12×12 Å³ was used, large enough to prevent the overlap of localized basis functions. The charge density was expanded in a grid of 150×150×150 points, corresponding to a plane-wave cutoff of 430 Ry, and the Hartree potential was obtained by fast Fourier transformation.

In our present study as well as in those by Oda *et al.* and Hobbs *et al.*, a calculation constrained to a unique magnetization direction, i.e. a collinear one, unavoidably resulted in a stable ferromagnetic solution. Relaxing the collinearity condition, again consistently with previous calculations, reliably reproduces a canted (in opposite directions) configuration of magnetic moments on two apical atoms, with respect to basal atoms whose moments remain parallel. The energy gain due to forming a canted structure lies in between the estimations done with the LDA in Refs. 19 and 20, closer to the latter. The values of local magnetic moments of all five atoms are very close, with the basal moments slightly higher in all cases of non-collinear structures considered. The absolute values of local magnetic moments depend on definition: in Ref. 20, the magnetization density was projected onto a sphere with radius 1.2 Å, whereas in our calculation, the Mulliken population analysis has been done for (strictly localized) basis functions. The total magnetic moment obtained in our calculation with the GGA is 18 μ_B , consistently with the result of Hobbs *et al.*²⁰. The same total magnetic moment was obtained in the LDA; the equilibrium interatomic distances were however noticeably reduced as compared to the GGA (Table I). The diagram of broadened energy levels (Fig. 3) shows that an accidental near degeneracy of two states with opposite spin direction occurs at the Fermi level, but is removed both in the GGA and by allowing non-collinear spin arrangement in the LDA. The differences in the energy level structure from the LDA and GGA calculations seen in Fig. 3 are in part due to differences in relaxed geometry and in part due to the exchange-correlation potential as such. GGA tends to produce larger separation between centers of gravity of majority-spin and minority-spin states than LDA does. The effect of geometry is primarily manifested in rearranging the levels in the vicinity of the Fermi level, aimed at reducing the band energy.

It is difficult to estimate *a priori* which part of existing differences from earlier calculations has to do with certain limitations of SIESTA, like the compactness of its localized basis set, and what can be due to other technical differences, like the construction and treatment of pseudopotentials. From one side, planewave methods allow a systematic enhancement of the basis set completeness; on the other side, the use of pseudopotential presumes certain compromise between its softness and transferability, not trivial in relation to transition metals, or anyway ambiguities in its construction (even in case of ultrasoft pseudopotentials⁴¹). We recall that the use of SIESTA, contrary to planewave methods, does not necessarily presume the pseudopotential to be soft – although that is normally advantageous.

In order to bring in some systematics in the analysis of our LDA and GGA results, we performed a sequence of fixed spin moment calculations, 12 to 20 μ_B , everywhere allowing for full structural relaxation. While the fixed spin moment of 18 μ_B yielded the ground state in both LDA and GGA cases, the total energy of the (next) $M=16 \mu_B$ state is higher by only 38 meV/at. in the LDA calculation (110 meV/at. in the GGA). Actually, even the next-stable structure with the fixed spin moment of 14 μ_B is not so much higher in energy than the ground state (74 meV/at.). Therefore the fact that it materialized as the LDA ground state in two previous planewave calculations^{19,20} seems plausible, in view of technical differences in implementing the LDA. On the contrary, the GGA solution with the total moment of 18 μ_B corresponds to a deep energy minimum, unambiguously found in both our calculation and that by Hobbs *et al.*²⁰. The variation of local magnetic moments and interatomic distances over different fixed-moment states is shown in Fig. 4. First we note that with the total magnetic moment forced to be 14 μ_B in the LDA calculation, our relaxed interatomic distances are indeed very close to those of Ref. 19,20. Moreover it is instructive to discuss the evolution of the structure and of local magnetic moments depending on the total fixed moment. It is understandable that larger interatomic distances are needed, on the average, to support larger total moments. However, basal-basal and basal-apical distances grow with the magnitude of the fixed spin moment at different rate. First the apical atoms

TABLE I: Structure and magnetic properties of the Fe₅ cluster (trigonal bipyramide) from SIESTA calculations and from the literature. Subscript b refers to basal Fe atoms, a – to apical ones. Interatomic distances a_{b-b} , a_{b-a} are in Å, magnetic moments M in μ_B . ΔE (meV) is difference in binding energy per atom between ferromagnetic and non-collinear configurations.

	a_{b-b}	a_{b-a}	M_b	M_a	canting M_a	M_{tot}	ΔE
present calculation							
coll. GGA (FM)	2.46	2.38	3.64	3.54	–	18.00	
coll. LDA (FM)	2.36	2.31	3.63	3.56	–	18.00	
non-coll. LDA	2.34	2.27	3.40	3.32	40.6°	15.24	25
Oda <i>et al.</i> ¹⁹							
coll. LDA (FM)	2.37	2.22	2.58	2.55	–	14.00	
non-coll. LDA	2.34	2.25	2.72	2.71	29.7°	14.57	10
Hobbs <i>et al.</i> ²⁰							
coll. GGA (FM)	2.39	2.34	3.11	3.17	–	18.00	
non-coll. GGA	2.38	2.33	3.04	2.71	31.3°	15.9	14
coll. LDA (FM)	2.34	2.24	2.80	2.85	–	14.00	
non-coll. LDA	2.33	2.24	2.87	2.83	35.9°	14.5	32

move away from a roughly fixed triangular base (whereby their local magnetic moments get a sharp increase); near $18 \mu_B$ the distance between apical and basal atoms gets stabilized, and the basal triangle grows further, as the main effect (in both LDA and GGA cases).

A more detailed insight into the composition of hybridized electronic states in cluster reveals the following. As the (fixed) total spin moment M augments, the majority-spin occupation numbers steadily grow, maintaining on all atoms roughly the same magnitude. Their minority-spin counterparts behave differently – some of them drop down by $0.15\text{--}0.2 e$, when corresponding hybridized states float upwards of the Fermi level. Thus, from $M=14$ to $16 \mu_B$ the $d_{x^2-y^2}$ occupation at the apical atoms drops simultaneously with the d_{xz} of basal atoms. This is accompanied by the increase of the apical-basal bond length. Further on, between $M=18$ and $20 \mu_B$ the minority-spin d_{z^2} occupation of the basal atoms drops down, that loosens the bonding within the basal triangle (see Fig. 4). For $M < 16 \mu_B$ and $M > 18 \mu_B$, local magnetic moments of apical atoms grow faster than those of basal atoms. It is noteworthy that the ground-state structure materializes when both local magnetic moments, on one side, and nearest-neighbor distances, on the other side, become “balanced” over the cluster.

In a recent study, Kortus *et al.*¹⁷ calculated equilibrium structure and magnetic properties of the Fe_5 cluster and found the ground-state magnetic moment of $16 \mu_B$ (with the GGA). They attribute the difference from our present results (and those by Hobbs²⁰) to the use of pseudopotentials, emphasizing at the same time good agreement of their data with earlier all-electron calculation by Castro *et al.*¹⁶. However, in view of the closeness of computational schemes applied in these two all-electron calculations (Gaussian-type orbitals as basis functions), one may wish to perform yet another study by a different all-electron method, in order to finally clarify the issue.

Our calculation setup can probably be further optimized for Fe systems by tuning the pseudopotential and extending the basis. So far, we managed to demonstrate that quite sensitive energetic and structural characteristics of Fe clusters can be reproduced by a SIESTA method at a quite moderate computational cost. Our next objective is the simulation of larger Fe particles for which, to our knowledge, structural relaxation has not yet been done.

V. ICOSAHEDRAL VS. FCC CLUSTERS

Clusters of icosahedral symmetry (*i*-) often come into discussion for noble gases, simple metals and also transition metals. In the present study, we simulated Fe_{13} and Fe_{55} *i*-particles as counterparts of fcc-structured clusters of corresponding size. Earlier results on *i*- Fe_{13} have been published by Kortus *et al.*¹⁷, and (among a number of isomers of $\text{Fe}_2 - \text{Fe}_{17}$ clusters) – by Diéguez *et al.*²⁹. Duan and Zhang²³ calculated electronic structure of 13-at. and 55-at. icosahedral clusters of Fe, Co, and Ni by the discrete variational method, and made a comparison with the results for fcc-type and hexagonal isomers. For 13-at. clusters they optimized the cluster radius; the results for the 55-at. iron cluster correspond to the interatomic distance fixed at that of bulk bcc iron. Nevertheless some trends reported in Ref. 23 hold in a relaxed geometry and are discussed below.

Our calculation for the *i*- Fe_{13} in the GGA lead to a structure with the total magnetic moment of $44 \mu_B$, that is identical to the all-electron result of Ref. 17. According to Duan and Zhang²³, the total moment is $46 \mu_B$. We find a local magnetic moment $2.78 \mu_B$ on the central atom, and $3.43 \mu_B$ – on its neighbors (separated by 2.43 \AA from the central one). The bond length as relaxed in Ref. 23 with the LDA is slightly smaller – 2.38 \AA (as could be generally expected in the LDA, that is known to overestimate the binding). Differently to Ref. 17 that reported an energy gap of 0.2 eV , the gap of only 0.05 eV was found in our case (in the minority-spin subband, fully within a much larger gap of 0.6 eV in the majority-spin states). The LDA calculation resulted in a smaller total moment of $36 \mu_B$ in a somehow compressed (2.30 \AA between central and peripheric atoms) cluster. The local magnetic moment of the central atom collapses to $0.93 \mu_B$. This makes a big difference to the previously cited LDA result of Ref. 23 in what regards both the magnetization and the bond length. Such disagreement is an indication that several metastable states of comparable energy exist for the *i*- Fe_{13} cluster, whereby the choice of one or another happens due to minute differences in the calculation setup, probably different starting conditions etc. A more systematic study could be done as a sequence of fixed-moment calculations, as discussed above for the Fe_5 cluster. It is noteworthy that the recent study by the same SIESTA method with only minutely different calculation setup²⁹ indicated the icosahedral cluster with not just reduced but actually inverted magnetization of the central atom (and total moment $34 \mu_B$) as the ground-state structure among several competing isomers (all treated in the LDA only). Such scattering of calculation results could be a good indication that collinear ordering of local magnetic moments becomes unstable. We tried to allow for non-collinear spin structure at least for the Fe_{13} cluster, but failed so far to arrive at a reliably converged magnetic configuration within a reasonable calculation time.

The tendency for the reduction (or inversion) of the central magnetic moment in the icosahedral environment becomes more pronounced in a larger Fe_{55} cluster. The magnetic moment of the central atom gets inverted ($-0.19 \mu_B$) even in the GGA calculation, that otherwise favours ferromagnetic structure as we have seen above. Note that Duan and Zheng²³ also obtained an inverted spin moment on the central atom in their (unrelaxed) *i*- Fe_{55} cluster, as

calculated with the LDA. The magnetic moments in the inner icosahedral shell are in our case suppressed to $\sim 0.34 \mu_B$, and the moments in the outer shell reach merely $1.97 \mu_B$ (for thirty 8-coordinated mid-edge atoms) to $2.25 \mu_B$ (twelve 6-coordinated vertex atoms). The qualitative trend of how magnetic moments change over icosahedral shells agrees with the results of Ref. 23. The difference in absolute numbers can be related to a substantial compression we find in the relaxed cluster. The radius of the inner shell shrinks to 2.4 \AA , i.e. by about 5% if compared to the equilibrium interatomic spacing in crystal. In the case of fcc structure, such decrease in volume would change the ferromagnetic high-spin state into one of competing antiferromagnetic arrangements as, e.g., Ref. 38 shows, or probably in a more complicated non-collinear structure, with moderate local moments. The relaxed radii of next spheres are about 4.2 \AA (30 atoms) and 4.9 \AA (12 atoms). Duan and Zheng²³ did not take inner compression in their *i*-cluster into account, that explains larger values of magnetic moments they obtained.

One can conclude therefore that *i*-clusters do actually demand for additional studies, where all existing ambiguities (ferromagnetic vs. ferrimagnetic ordering, GGA vs. LDA) will be analyzed on a more systematic basis, like e.g. running a sequence of fixed-spin-moment calculations. In principle one could expect the presence of several structural solutions for some total moment numbers.

VI. LARGER BCC AND FCC-STRUCTURED CLUSTERS

The study of morphology and magnetic ordering of small clusters is a delicate matter, sensitive to the calculation details and prone to computational instabilities. Corresponding results are accessible from experiment rather indirectly. In larger metal nanoparticles (from $\sim 10^2$ atoms on), ordered structures are often detected by electron microscopy studies, so that substantial deviations from crystalline behavior remain constrained to a (more or less thick) surface layer. The aim of our further study was to simulate structure relaxation and radial distribution of magnetic moments inside Fe particles with several tens of atoms. Calculations for bcc-related Fe_{15} and Fe_{35} clusters, albeit without structure relaxation, have been reported by Fujima and Yamaguchi²² (in a row of Ni and Cr clusters of comparable size). Therefore we address in the following primarily the fcc-related clusters, including Fe_{35} for comparison. We considered particles having either a central atom, or centered around an octahedral interstitial, and allowed unconstrained structure relaxation after introducing small off-center displacements. The relaxed structure essentially preserved the cubic point symmetry, with the exception of the AFM (of CuAu-type) Fe_{62} particle that developed a slight tetragonal distortion. The (relaxed) radii of atomic shells along with corresponding magnetic moments are presented in Table II. All these results are obtained in the GGA. The values of local magnetic moments per atom are estimated from the Mulliken population analysis. The values to be compared to in perfect relaxed crystal, according to the SIESTA calculation, are $2.43 \mu_B$ (fcc) and $2.35 \mu_B$ (bcc). We show schematically the variation of magnetic moments over relaxed spheres of neighbors in Fig. 5 (for particles formed around an octahedral interstitial) and Fig. 6 (for particles with a central atom).

The comparison of unrelaxed bulk-like bcc geometry with the final relaxed structure helps to attribute the drop of the magnetic moment in the first (8-at.) coordination shell around the central atom in the (bcc) Fe_{35} cluster, found by Fujima and Yamaguchi²², to the structure effect (and not, say, to the differences in the calculation scheme or in the definition of local magnetic moments). If the neighbors' positions are fixed as in the bulk, the local magnetic moments are 2.31 (on the central atom); 2.21; 2.98; 3.23 and 3.45 (on the surface) μ_B , i.e. the drop in the magnetic moment of the second shell is reproduced. However, with full relaxation taken into account in the Fe_{35} cluster, we found the magnetic moment to grow steadily towards the surface (see Fig. 6, Table II). This effect seems to be intrinsic to the bcc morphology since we again find it in a larger Fe_{59} cluster: the inward relaxation of the atoms in the first coordination shell gradually increases their local magnetic moments. In this process, the radii of 8-at. and 6-at. coordination spheres, whose relation in the bulk is nearly 0.87, become pronouncedly separated in clusters, reducing the above ratio to 0.77 in Fe_{35} and 0.79 in Fe_{59} (see Fig. 6, bottom panel).

Consistently with the results of Ref. 22, the magnetic moments grow in the outer shells and exceed $3 \mu_B$ on the surface. The remaining quantitative differences between our results for the Fe_{35} cluster and those by Fujima and Yamaguchi²² can be due to different exchange-correlation potential (X_α used in Ref. 22). The relaxation (neglected in Ref. 22) is outwards for the second shell (6 atoms) and inwards in all others. We found (this applies to the fcc clusters as well) the inward relaxation to be the largest on the surface, where the magnetic moment is at most enhanced. This behaviour is in consistence with well-known trends at the surface of bulk Fe. The enhancement of *local* magnetic moments (i.e., inside muffin-tin spheres) in the slab full-potential calculation was found by Freeman and Fu⁴² to be from $2.15 \mu_B$ (bulk) to $2.65 \mu_B$ at the (110) surface and $2.98 \mu_B$ at the (100) surface. The surface relaxation (see, e.g., a recent first-principle calculation by Spencer *et al.*⁴³, that also reviews experimental results for different Fe surfaces) is always inwards for the upper layer.

In the fcc-related clusters, the internal structure is more densely packed, and a pronounced outward relaxation occurs for the second shell (6 at.) of the atom-centered Fe_{43} cluster. Comparing this to the result for the (interstitial-

centered) Fe₆₂ cluster, one sees moreover a general tendency of developing a (quite small) outward relaxation in the subsurface shell, whereas the outer shell is always strongly contracted. Towards further inner shells, the relaxation is rapidly stabilized, and the atomic spacing approaches that in the bulk. As in the case of the bcc cluster, magnetic moments are largely enhanced on the surface (and immediately below it), but rapidly decrease and get stabilized in the deeper shells, without showing any fluctuations. Such behaviour agrees qualitatively with the results of Duan and Zheng²³ on the fcc Fe₅₅ cluster, done however with fixed interatomic distances (equal to those in the bcc bulk). We do not find any clear reversal of magnetization on the central atom of the fcc Fe₅₅ cluster, in contrary to what was reported in Ref. 23. One cannot exclude the possibility for such a configuration to emerge in one of metastable states, in a calculation departing from a specially prepared initial magnetic configuration. However, whereas AFM and FM types of ordering are known to be competitive in fcc Fe, on the high-spin side (large volumes) the FM arrangement is definitely more favourable, at least in the bulk³⁸. Moreover, experimental estimates of mean magnetic moments for the Fe₅₅ cluster (3.1 μ_B , according to Ref. 1) are in better agreement with our result of 2.77 μ_B than with 2.58 μ_B after Duan and Zheng²³.

An additional study of the plausibility of AFM ordering was undertaken for the Fe₆₂ cluster. The layer-by-layer (i.e., CuAu-type) AFM organization lifts some degeneracies in the radial distribution of atoms (see Fig. 5), but otherwise is consistent with the above observations (inward surface relaxation; enhancement of magnetic moments towards the surface). The total energy per atom is by 0.19 eV higher in the AFM configuration than in the corresponding FM case, that effectively rules out this particular (admittedly arbitrary) magnetic configuration as a competitive one. However, the fact that the magnitudes of magnetic moments over shells are almost identical in AFM and FM cases implies that the individual spins are localized enough to survive in different magnetic orientations, and could probably prove a gain in the magnetic energy in some of them.

It could be instructive to analyze how the enhanced magnetization at the surface decomposes into contributions from different basis orbitals, and how the electron density gets distributed between the inner part and the surface of clusters in the course of relaxation. Fortunately one can establish very clear trends, common for fcc and bcc clusters of different size. Magnetic polarization of the 4s states is in all cases well below 0.1 μ_B and antiparallel to the magnetic moment in the 3d shell. It gradually disappears (to about 0.01 μ_B) towards the surface. This is consistent with the magnetic moment decomposition for the Fe₅₅ cluster by Duan and Zheng²³. In disagreement with the latter, we find that the polarization in the 4p shells, being parallel to that of 3d, steadily increases from the core region outwards and contributes as much as 7% of local magnetic moments at the surface. The major, 3d-related, part of the local moment grows due to simultaneous increase of majority-spin and decrease of minority-spin occupations. However, the majority-spin 3d subband never gets saturated (in fact, its occupation does not exceed 4.8 electrons). The charge transfer always happen from the core region to the surface; the nominal valence charge per Fe atom is 7.4–7.6 in the

TABLE II: Relaxed distances from center a and magnetic moments over shells of neighbors M in bcc- and fcc-related Fe clusters. Numbers of neighbors within each shell are given in parentheses.

	a (Å)	M (μ_B)		a (Å)	M (μ_B)
	Fe ₃₅ (bcc)			Fe ₅₉ (bcc)	
(1)	0.0	2.10	(1)	0.0	2.85
(8)	2.345	2.14	(8)	2.525	2.64
(6)	3.043	3.13	(6)	3.202	2.45
(12)	3.880	3.21	(12)	4.026	2.79
(8)	4.603	3.43	(24)	4.678	3.25
	Fe ₃₈ (fcc)		(8)	4.821	3.13
(6)	1.827	2.62		Fe ₆₂ (fcc)	
(8)	3.281	2.90	(6)	1.857	2.41
(24)	3.985	3.14	(8)	3.082	2.52
	Fe ₄₃ (fcc)		(24)	4.173	2.93
(1)	0.0	2.45	(24)	5.245	3.21
(12)	2.579	2.52		Fe ₆₂ (fcc), AFM	
(6)	3.798	3.00	(4)	1.767	1.45
(24)	4.307	3.22	(2)	1.877	-2.35
	Fe ₅₅ (fcc)		(8)	3.086	-1.82
(1)	0.0	2.29	(8)	3.883	-2.43
(12)	2.507	2.26	(8)	4.029	3.04
(6)	3.361	2.73	(8)	4.150	-2.79
(24)	4.124	2.85	(16)	5.262	-3.25
(12)	4.797	3.17	(8)	5.294	3.46

cluster core and slightly beyond 8 at the surface. As definition-dependent as these qualitative estimates might be, they do not let to oversee a general qualitative trend. Duan and Zheng²³ found fluctuations of charge from one atom shell to another, but on the average no clear distinction between core and surface atoms – hence the difference we talk about must come from relaxation, taken into account in our case. It is understandable that the overall compression in the cluster due to its “surface tension” shifts upwards the electron states in the inner region, that results in the outward charge flow. Surface atoms experience stronger relaxation but they have lower coordination. The atoms adjust in the cluster so as to smooth the radial charge distribution; simultaneously the magnetization profile tends to acquire certain regularity. The enhancement of the $4p$ contribution to the magnetic polarization on the surface is related with the abovementioned redistribution of charge, because extra electrons in the surface layer can be more easily accommodated by majority-spin states of the p symmetry.

According to the experimental evidence^{1,2}, average magnetic moments per atom start from nearly $3 \mu_B$ in small clusters and gradually decrease to the bulk value of $2.2 \mu_B$ in 400–500 atom particles. This implies ferromagnetic ordering and bcc-related structure in large clusters. The fluctuations of magnetization prior to this asymptotic value being achieved are not yet systematically explained. Billas *et al.* emphasize¹ that the mean magnetic moment in the Fe_{55} atom is anomalously large (nearly $3.1 \mu_B$), and bring the icosahedral structure into discussion. However, we have seen that the $i\text{-Fe}_{55}$ cluster has in fact a moderate mean magnetic moment of $2.2 \mu_B$ (or slightly larger, but anyway well below that of the fcc cluster, in Ref. 23). In order to describe experimental variations of mean magnetic moments in simple terms, Billas *et al.* proposed² a model of Fe magnetic moments decreasing from the surface into the interior of the cluster, and getting inverted in the fourth shell from the surface. While essentially confirming this model in what concerns the asymptotic end values of magnetic moments (on the surface and in the bcc interior), our simulation does not yet produce any strong evidence for the fluctuations in between, when starting from ferromagnetic test configuration. However, a more detailed analysis (e.g., within a fixed spin moment scheme) could help to single out other competing magnetic structures.

Addressing the issue of structural order vs. disorder, it is worth noting that Soler *et al.*²⁷ studied the morphology of small (38 to 75 atoms) “ordered” and “amorphous” gold nanoparticles, using the same calculation scheme as here in order to refine trial geometries, provided by energy minimization in an empirical potential. In all cases “amorphous” particles were found to be more stable, and the subsequent analysis shows the reason for this to be due to high elastic contribution to the total energy of a particle, relaxed in the course of an amorphous-like rearrangement of atoms. In our case, inner shells of Fe particles are also contracted, as compared to the bulk crystal. It would be interesting to probe the effects of amorphization, and their interplay with magnetic characteristics, in an *ab initio* simulation once realistic models for ground-state Fe arrangements become available.

Summarizing, our results favors a conclusion that the relaxation and magnetic properties of small Fe nanoparticles have certain common features, relatively independent on morphology, magnetic ordering and size. Namely, the structure relaxation is practically confined within 2–3 outer shells, the surface layer relaxes strongly inward, and the magnetic moments on the surface are enhanced to beyond $3 \mu_B$. The overall magnetic properties of larger nanoparticles must be then primarily governed by the proportion between surface-layers atoms and their deep bulk-like counterparts.

Acknowledgments

The work was supported by the German Research Society (SFB 445) and by Spain’s Fundación Ramón Areces and MCyT (BFM2000-1312). The authors are grateful to L. C. Balbás and P. Ordejón for useful discussions. JMS thanks J. Kübler and R. Martin for their help in the development of the non-collinear magnetization option in SIESTA. AVP thanks J. Kortus for useful discussions on the subject of small Fe clusters.

* Electronic address: postnik@thp.uni-duisburg.de

† Electronic address: entel@thp.uni-duisburg.de

‡ Electronic address: jose.soler@uam.es

¹ I. M. L. Billas, J. A. Becker, A. Châtelain, and W. A. de Heer, *Phys. Rev. Lett.* **71**, 4067 (1993).

² I. M. L. Billas, A. Châtelain, and W. A. de Heer, *Science* **265**, 1682 (1994).

³ D. Gerion, A. Hirt, I. M. L. Billas, A. Châtelain, and W. A. de Heer, *Phys. Rev. B* **62**, 7491 (2000).

⁴ O. B. Christensen and M. L. Cohen, *Phys. Rev. B* **47**, 13643 (1993).

⁵ N. A. Besley, R. L. Johnston, A. J. Stace, and J. Uppenbrink, *Journal of Molecular Structure (Theochem)* **341**, 75 (1995).

⁶ G. M. Pastor, J. Dorantes-Dávila, and K. H. Bennemann, *Phys. Rev. B* **40**, 7642 (1989).

⁷ G. M. Pastor, R. Hirsch, and B. Mühlischlegel, *Phys. Rev. B* **53**, 10382 (1996).

⁸ A. N. Andriotis, N. Lathiotakis, and M. Menon, *Chem. Phys. Lett.* **260**, 15 (1996).

- ⁹ A. N. Andriotis, N. N. Lathiotakis, and M. Menon, *Europhys. Lett.* **36**, 37 (1996).
- ¹⁰ A. N. Andriotis and M. Menon, *Phys. Rev. B* **57**, 10069 (1998).
- ¹¹ S. Bouarab, A. Vega, J. A. Alonso, and M. P. Iñiguez, *Phys. Rev. B* **54**, 3003 (1996).
- ¹² J. Guevara, F. Parisi, A. M. Llois, and M. Weissmann, *Phys. Rev. B* **55**, 13283 (1997).
- ¹³ W. Kohn, *Rev. Mod. Phys.* **71**, 1253 (1999).
- ¹⁴ J. L. Chen, C. S. Wang, K. A. Jackson, and M. R. Pederson, *Phys. Rev. B* **44**, 6558 (1991).
- ¹⁵ M. Castro and D. R. Salahub, *Phys. Rev. B* **49**, 11842 (1994).
- ¹⁶ M. Castro, C. Jamorski, and D. R. Salahub, *Chem. Phys. Lett.* **271**, 133 (1997).
- ¹⁷ J. Kortus, T. Baruah, M. R. Pederson, C. Ashman, and S. N. Khanna, *Appl. Phys. Lett.* **80**, 4193 (2002).
- ¹⁸ P. Ballone and R. O. Jones, *Chem. Phys. Lett.* **233**, 632 (1995).
- ¹⁹ T. Oda, A. Pasquarello, and R. Car, *Phys. Rev. Lett.* **80**, 3622 (1998).
- ²⁰ D. Hobbs, G. Kresse, and J. Hafner, *Phys. Rev. B* **62**, 11556 (2000).
- ²¹ J. A. Alonso, *Chem. Rev.* **100**, 637 (2000).
- ²² N. Fujima and T. Yamaguchi, *Materials Science and Engineering A* **217–218**, 295 (1996).
- ²³ H. M. Duan and Q. Q. Zheng, *Phys. Lett. A* **280**, 333 (2001).
- ²⁴ D. Sánchez-Portal, P. Ordejón, E. Artacho, and J. M. Soler, *Int. J. Quant. Chem.* **65**, 453 (1997).
- ²⁵ E. Artacho, D. Sánchez-Portal, P. Ordejón, A. García, and J. M. Soler, *Physica Status Solidi (b)* **215**, 809 (1999).
- ²⁶ J. M. Soler, E. Artacho, J. D. Gale, A. García, J. Junquera, P. Ordejón, and D. Sánchez-Portal, *J. Phys.: Condens. Matter* **14**, 2745 (2002).
- ²⁷ J. M. Soler, M. R. Beltrán, K. Michaelian, I. L. Garzón, P. Ordejón, D. Sánchez-Portal, and E. Artacho, *Phys. Rev. B* **61**, 5771 (2000).
- ²⁸ J. Izquierdo, A. Vega, L. C. Balbás, D. Sánchez-Portal, J. Junquera, E. Artacho, J. M. Soler, and P. Ordejón, *Phys. Rev. B* **61**, 13639 (2000).
- ²⁹ O. Diéguez, M. M. G. Alemany, C. Rey, P. Ordejón, and L. J. Gallego, *Phys. Rev. B* **63**, 205407 (2001).
- ³⁰ P. Ordejón, D. A. Drabold, R. M. Martin, and M. P. Grumbach, *Phys. Rev. B* **51**, 1456 (1995).
- ³¹ P. Ordejón, E. Artacho, and J. M. Soler, *Phys. Rev. B* **53**, R10441 (1996).
- ³² S. G. Louie, S. Froyen, and M. L. Cohen, *Phys. Rev. B* **26**, 1738 (1982).
- ³³ We learned that Diéguez *et al.* found similar results with a basis like ours. Larger extension of basis function is primarily essential for precise evaluation of formation energies and less important for geometry optimizations (P. Ordejón, private communication).
- ³⁴ V. L. Moruzzi, P. M. Marcus, K. Schwarz, and P. Mohn, *Phys. Rev. B* **34**, 1784 (1986).
- ³⁵ V. L. Moruzzi, *Phys. Rev. Lett.* **57**, 2211 (1986).
- ³⁶ P. Bagno, O. Jepsen, and O. Gunnarsson, *Phys. Rev. B* **40**, 1997 (1989).
- ³⁷ T. C. Leung, C. T. Chan, and B. N. Harmon, *Phys. Rev. B* **44**, 2923 (1991).
- ³⁸ H. C. Herper, E. Hoffmann, and P. Entel, *Phys. Rev. B* **60**, 3839 (1999).
- ³⁹ P. Blaha, K. Schwarz, G. K. H. Madsen, D. Kvasnicka, and J. Luitz, *WIEN2k, Vienna University of Technology* (2001), improved and updated Unix version of the original copyrighted WIEN-code, which was published by P. Blaha, K. Schwarz, P. Sorantin, and S. B. Trickey, in *Comput. Phys. Commun.* **59**, 339 (1990), URL <http://www.wien2k.at>.
- ⁴⁰ J. P. Perdew, K. Burke, and M. Ernzerhof, *Phys. Rev. Lett.* **77**, 3865 (1996).
- ⁴¹ Of the methods applied so far for the study of small clusters, the projector augmented-wave method as used in Ref. 20 has potentially the superior accuracy, as it is an all-electron one and allows to enhance the completeness of the basis in a systematic way. However, the use of frozen core approximation in actual calculations so far keeps its level of accuracy still somehow inferior to, say, FLAPW. The disagreement with accurate all-electron results obtained by a Gaussian-type orbital method for the Fe₅ cluster in Ref. 17 is not yet understood.
- ⁴² A. J. Freeman and C. L. Fu, *J. Appl. Physics* **61**, 3356 (1987).
- ⁴³ M. J. S. Spencer, A. Hung, I. K. Snook, and I. Yarovsky, *Surf. Sci.* **513**, 389 (2002).

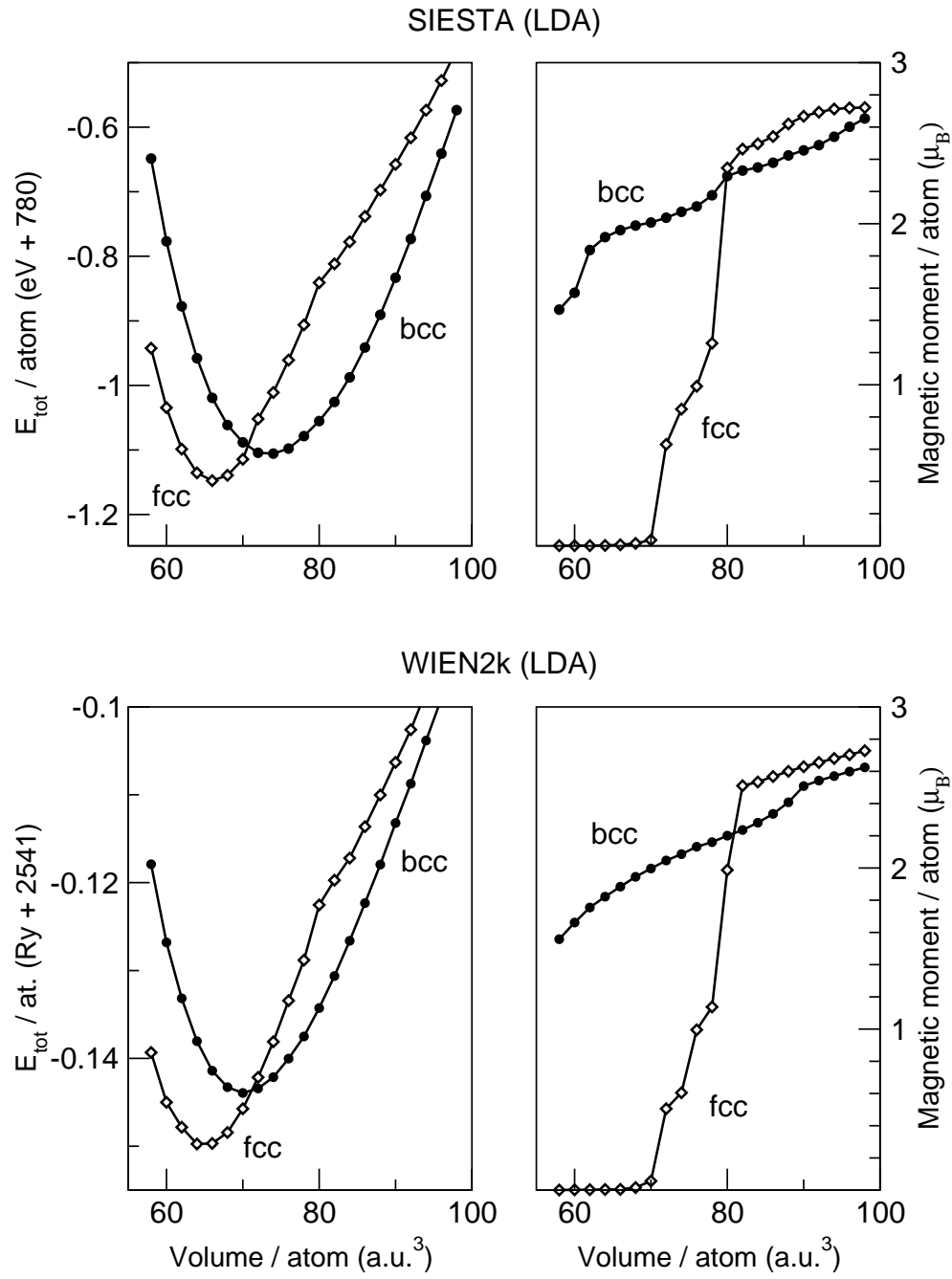


FIG. 1: Total energy vs. volume (left panel) and magnetic moment per atom (right panel) for fcc and bcc phases as calculated with SIESTA (top) and WIEN2k (bottom) in the local density approximation. Brillouin zone integration in SIESTA was done by the Monkhorst-Pack method with $12 \times 12 \times 12$ divisions in the full Brillouin zone.

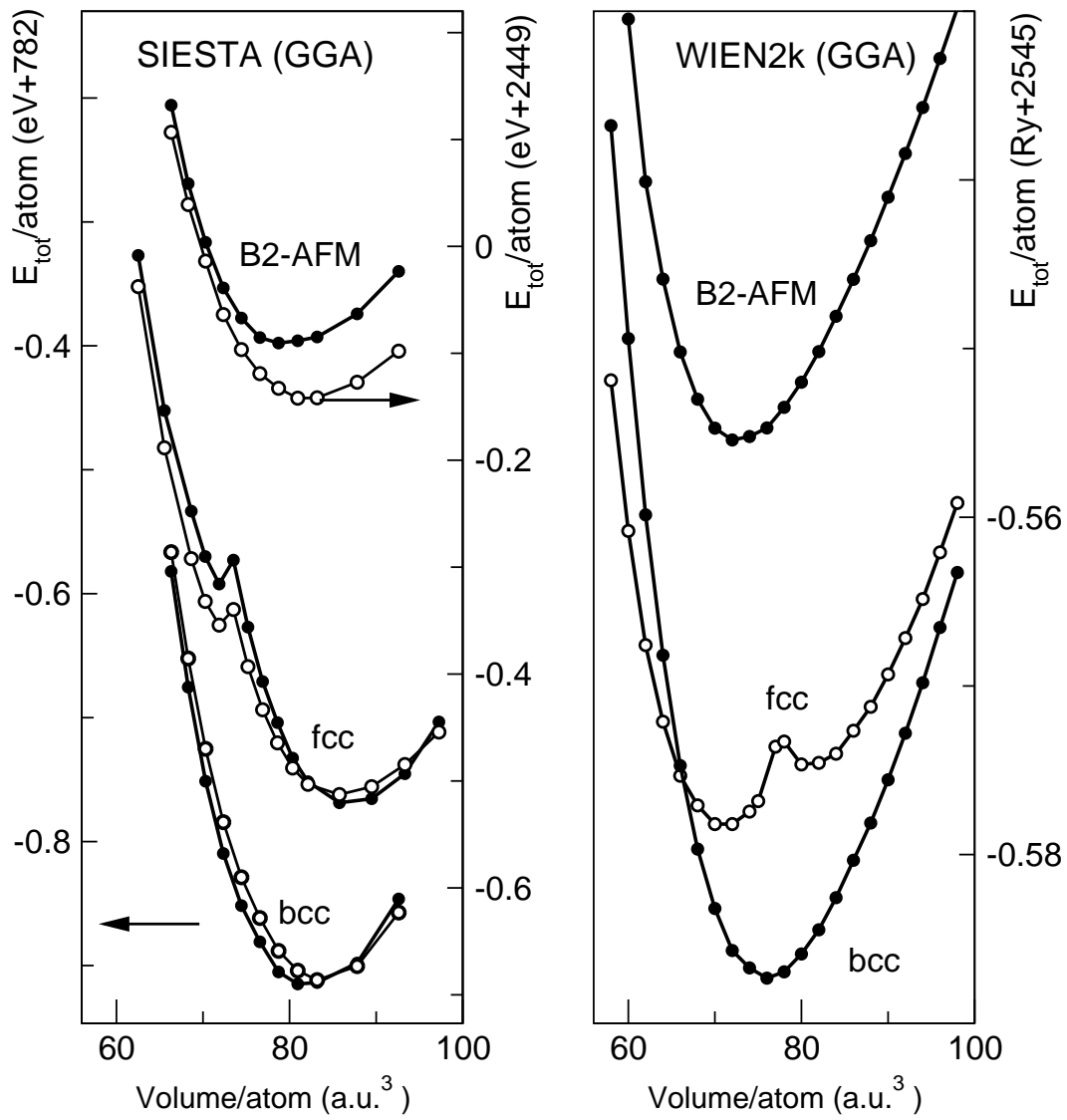


FIG. 2: Total energy vs. volume for ferromagnetic fcc and bcc and for the B2 antiferromagnetic phase, using generalized gradient approximation for exchange-correlation. Left panel: SIESTA calculation, with $3p$ states attributed to the core (black dots, left energy scale) or treated as valence states in the generation of norm-conserving pseudopotential (open dots, right energy scale). Right panel: all-electron calculation with the WIEN2k code.

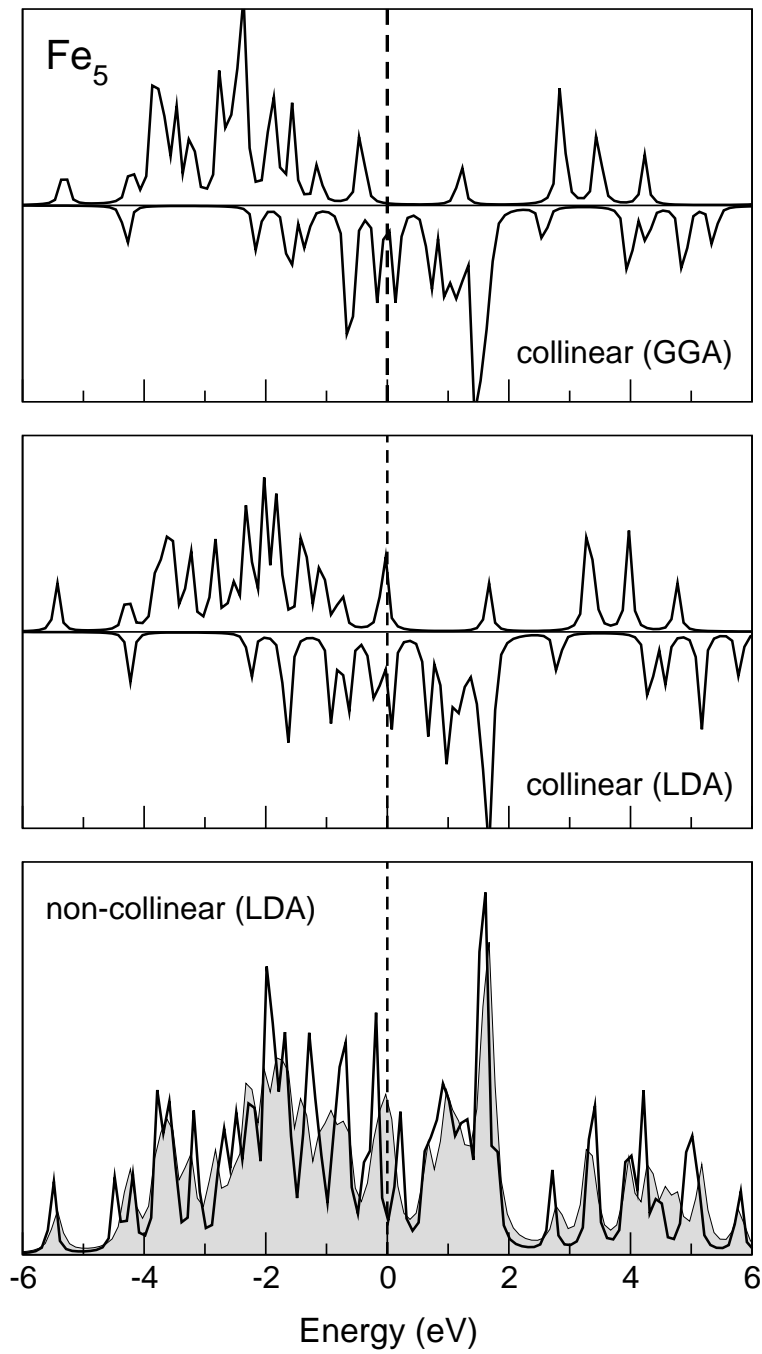


FIG. 3: Energy levels broadened by 0.1 eV in the Fe₅ cluster based on LDA and GGA calculations for ferromagnetic ordering (top and middle panels), and for the ground-state non-collinear structure (bottom panel). The results for the collinear case are resolved in majority-spin and minority-spin contributions. In the bottom panel, the collinear LDA result summed up over both spin channels is shown for comparison as shadowed area. Note the elevated density of states at the Fermi energy (=0 in the plot), removed by non-collinear spin arrangement.

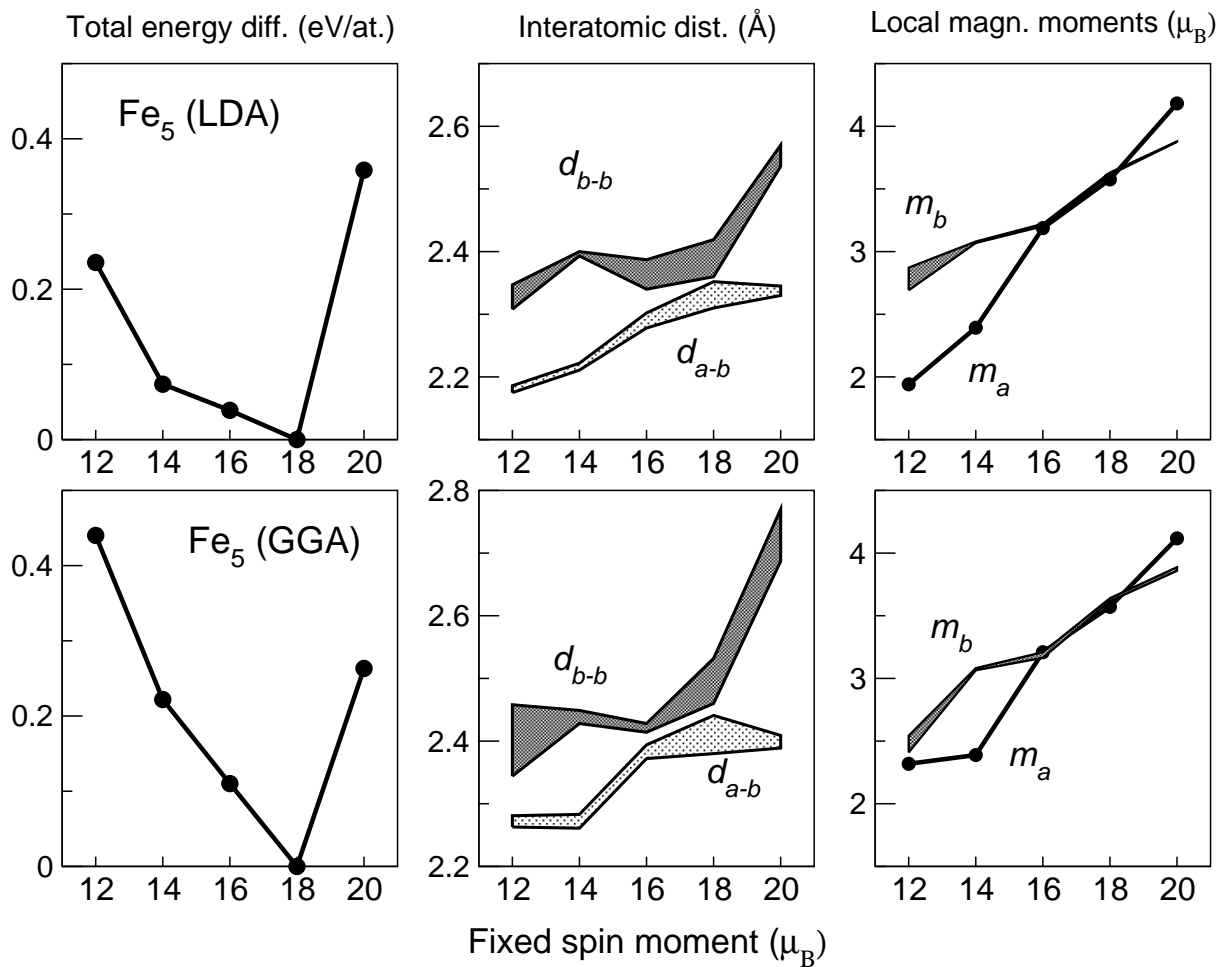


FIG. 4: Total energy (relative to the ground state), local magnetic moments M_b , M_a and interatomic distances d_{b-b} , d_{a-b} depending on the fixed spin moment as results of the LDA (upper row) and GGA (lower row) calculations for the Fe_5 cluster. Subscript b refers to basal Fe atoms, a – to apical ones. Shaded areas indicate variation of d or m within different atoms of the same type (a or b).

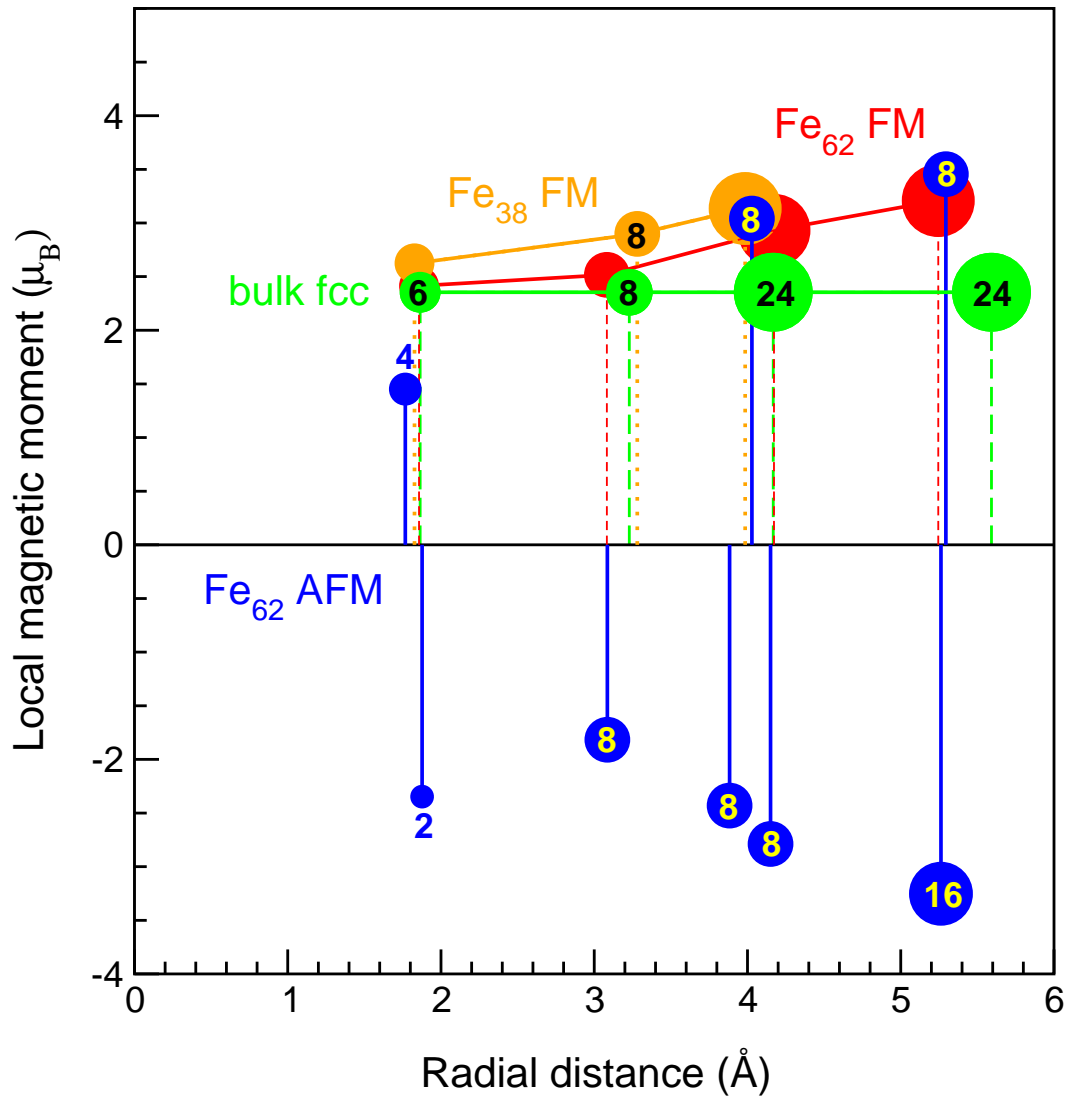


FIG. 5: Distribution of local magnetic moments over shells of neighbors in fcc-related nanoparticles Fe_{38} and Fe_{62} , centered around an octahedral interstitial. For the latter particle, results corresponding to FM and AFM ordering are shown. The size of the circle indicates the number of neighbors n in corresponding shell. The data for the fcc lattice are shown for comparison.

